

# A Distributed Autonomous System for Multi-UAVs With Limited Visualization: Employing Dual-Horizon NMPC Controller

JUN TANG 

YU WAN 

SONGYANG LAO

ZIPENG ZHAO

National University of Defense Technology, Changsha, China

Autonomous cooperative flight of multiple unmanned aerial vehicles (UAVs) in complex and unknown environments, such as jungles, poses significant challenges. Existing approaches often rely on wireless communication or omnidirectional vision to achieve cooperation. This article presents a dual-horizon nonlinear model-predictive control (NMPC) scheme for vision-limited multi-UAV systems in cluttered scenarios. The proposed scheme serves as a local path planner for UAVs equipped with forward vision limited to a 160° field of view, enabling distributed cooperative flight, obstacle avoidance, and navigation. To expand the observation area, UAVs randomly oscillate left and right around their direction of motion. The NMPC employs an objective function incorporating distributed cooperative flight and obstacle avoidance considerations during navigation. This objective function consists of short-term reactive objectives to maintain formation and consistent distance from neighbors and long-term predictive objectives for planning collision-free trajectories. CasADI, an open-source tool for nonlinear optimization and algorithmic differentiation, is utilized to solve the NMPC problem. The trajectory calculation is performed using initial conditions and fed as additional input to the NMPC. The first control signal of the predictive control sequence is then transmitted to the autopilot for UAV control. The proposed NMPC approach provides real-time solutions with a 10-Hz operating frequency and a 2-s prediction horizon, making it suitable as a local

Manuscript received 9 April 2023; revised 12 September 2023 and 11 January 2024; accepted 28 May 2024. Date of publication 11 June 2024; date of current version 11 October 2024.

DOI. No. 10.1109/TAES.2024.3411563

Refereeing of this contribution was handled by Andrea L’Afflitto.

This work was supported in part by the National Natural Science Foundation of China under Grant 62073330.

Authors’ address: Jun Tang, Yu Wan, Songyang Lao, and Zipeng Zhao are with the College of System Engineering, National University of Defense Technology, Changsha 410000, China, E-mail: (tangjun06@nudt.edu.cn; wanyu13@nudt.edu.cn; laosongyang@vip.sina.com; zhaozipeng22@nudt.edu.cn). (Jun Tang and Yu Wan are co-first authors.) (Corresponding author: Yu Wan.)

0018-9251 © 2024 IEEE

path planner. The effectiveness of the proposed approach is evaluated in three challenging scenarios using Gazebo-ROS.

## I. INTRODUCTION

Swarm technology for drones has gained significant attraction in both military and civilian applications due to its efficiency, convenience, flexibility, and low cost [1], [2]. While numerous proficient and expeditious multi-unmanned aerial vehicle (UAV) cooperative planners, reliant on wireless communication for static environments, have been proposed [3], [4], [5], the development of a real-time planner utilizing visual information remains an unresolved challenge in the field of control systems.

Current multi-UAV systems predominantly depend on data links for information sharing and coordination of complex behaviors. However, wireless communication has inherent limitations, such as distance, bandwidth, and reliability, which are exacerbated in complex environments. Issues such as data loss, communication delay, interference, network attacks, or even communication interruption and hijacking may arise [6], [7], [8].

In contrast, many biological groups, including birds, fish, and insects, display remarkable collective behaviors, such as coordinated migration, foraging, and predator avoidance, without relying on central control [9], [10], [11], [12]. Studies suggest that these groups primarily rely on visual information for interaction during collective decision making [13], [14]. As opposed to wireless communication, vision perception for drones offers numerous advantages, including information density and timeliness and anti-interference capabilities, especially in complex rejected environment. As a result, onboard cameras with low weight, cost, and size are progressively being employed in multi-UAV systems for situational awareness. Nevertheless, most of the existing collective models assume global visual information access for each agent [15], [16]. Biological studies have shown that birds’ eyeballs have a specific finite visual field rather than a global one and bird flocks exhibit better coordination under optimal constrained vision than under global vision [17], [18]. In reality, real-world drones typically have limited visual fields due to sensor and computing constraints. Some researchers have attempted to expand visual fields by increasing the number and layout of cameras, but this approach increases costs and demands on drone payload and computing power [19], [20]. Consequently, it is crucial to investigate multi-UAV swarms with limited vision.

For distributed multi-UAV systems, an effective planner is needed to enable each UAV to plan a dynamic, feasible, collision-free, and cooperative path under limited environmental perception. Inspired by natural swarming behavior, two primary methods have been explored: short-term reactive action and long-term smooth maneuvers [21], [22]. The former, influenced by insects, allows for rapid yet ephemeral responses to abrupt environmental alterations within a brief time frame. In contrast, the latter, inspired by birds, is well suited for more intricate and prolonged tasks, such as aerial

food search, intricate flight path planning, or accurate target tracking. Among these, the nonlinear model-predictive control (NMPC) approach to path planning, belonging to the latter, has gained increasing attention in the field of UAVs, due to its advantages in considering multiple constraints and optimizing trajectories in real time, thus enhancing efficiency and safety in complex environments [23], [24]. However, computation time remains a significant factor limiting its early development.

To address computation time issues and enable drones with a single onboard camera to achieve complex behaviors, such as cooperation, obstacle avoidance, and tracking in obstacle-dense environments, this article proposes an NMPC motion planner that integrates features of swarm behavior observed in both insects and birds. The objective function is composed of short-term reactive objectives and long-term smooth objectives. The former primarily focuses on maintaining a preferred distance from neighboring agents, preserving formation, and avoiding collisions. The latter considers the UAV's migration direction while avoiding obstacles. In addition, control effort is minimized to smoothen the trajectory and enhance energy efficiency. Each agent in the UAV swarm has a limited forward field of view, with only a forward camera. The agent randomly oscillates left and right around its own direction of motion to expand its observation area, ensuring the maximum visibility of nearby UAVs. To achieve real-time computation, we employ the open-source CasADI solver at a 10-Hz frequency. At each sampling moment, we solve an open-loop optimization problem within a finite-time interval based on the current state and transmit the first control signal of the predicted control sequence to the autopilot for controlling the drone's movement.

Our model incorporates two key innovations: a restricted visual field with a random line-of-sight (LOS) model and a dual-horizon NMPC controller. The main contributions of this article are as follows.

- 1) We consider a restricted visual field for each agent in the swarm, which is more realistic than most previous models that assume full or partial observability. To enhance each UAV's situational awareness, we introduce a random LOS model in which each agent oscillates periodically around its own direction of motion to expand its field of view.
- 2) We design a dual-horizon NMPC controller that decomposes the objective function into short-term reactive objectives and long-term planning objectives. The former considers the swarm's rapidly changing state to ensure cohesion, while the latter considers the stable migration direction and ensures safety with environmental obstacles. This controller can quickly and effectively adapt to changing situations under visual perception while generating collision-free trajectories. It also reduces computational burden and improves computational efficiency compared to conventional model-predictive control (MPC) controllers, allowing for real-time operation.

- 3) We implement a fully distributed and asynchronous system, where each UAV independently controls its motion based on local information obtained from its visual field. The multi-UAV system exhibits emergent order and can cooperatively achieve a common goal. This system is more efficient.
- 4) Unlike some existing models that simplify UAV dynamics as a particle, we model the UAV using the Robot Operating System (ROS) and Betaflight, validating the effectiveness of our algorithms through various challenging simulation scenarios in Gazebo. Our results indicate that our approach is capable of handling both simulated and realistic scenarios.

The rest of this article is organized as follows. Section II describes the related work. Section III details the proposed method. The effectiveness of the proposed method is verified by simulation experiments in Section IV. Finally, Section V concludes this article.

## II. RELATED WORK

This section discusses related work in the areas of multi-UAV motion control models, MPC-based motion controllers for UAVs, and a restricted vision model. We provide an overview of the relevant methods and challenges in each area and conclude with a brief summary.

### A. Multi-UAV Motion Control Model

Multi-UAV swarm motion control typically encompasses three primary aspects: formation control, path planning, and obstacle avoidance.

Formation control pertains to maintaining a desired geometric configuration among multiple UAVs, which can be either rigid or flexible. Rigid formations necessitate that UAVs maintain fixed relative positions and velocities concerning one another, while flexible formations permit UAVs to dynamically adjust their relative positions and velocities following specific rules, such as separation, alignment, and cohesion rules. Conventional methods for rigid formation control include leader-follower strategies [25], [26], [27], virtual structure approaches [27], [28], [29], and consensus methods [30], [31], [32], [33], [34]. Flexible formation control methods typically involve various swarm intelligence algorithms, such as Reynolds-Boids algorithm [35] and its revisions [3], [5], [19], [36], [37], [38]. Interagent communication and coordination are critical in achieving formation control in UAV swarm motion.

Path planning entails generating feasible trajectories for each UAV in the swarm that fulfill certain objectives, such as formation maintenance, reaching a target location, or minimizing energy consumption. It can be classified into different categories based on distinct criteria, including optimization-based or rule-based methods [21], [22]. Optimization-based methods formulate the planning problem as a constrained optimization problem that minimizes a specific cost function subject to constraints, such as collision avoidance and formation keeping [4], [39], [40], [41], [42]. Rule-based methods compute the control inputs for

each UAV based on predefined rules that capture desired behaviors, such as separation, alignment, and cohesion. The control inputs can be combined according to specific weights to obtain a desired velocity for each UAV. Some typical examples of rule-based methods include the artificial potential field method [43], the geometric method [44], and the Reynolds–Boids algorithm.

Obstacle avoidance is essential for each UAV in the swarm to prevent collisions with other UAVs or obstacles in the environment. While closely related to path planning, obstacle avoidance can be considered a separate aspect that emphasizes safety rather than optimality. Obstacles can be either static or dynamic, depending on their mobility, and either reactive or proactive, based on whether the UAVs plan ahead or react on the fly. Reactive collision avoidance generates an instantaneous velocity for each UAV when it encounters an obstacle, such as the artificial potential field method and the geometric method. Proactive collision avoidance generates a collision-free trajectory for each UAV by solving a constrained optimization problem. Collision avoidance can be achieved by applying hard constraints, which limit trajectories within specific convex spaces [40], [41], or soft constraints that incorporate penalty functions directly into the objective function [4].

## B. MPC-Based Motion Controller for UAVs

MPC is a widely studied control strategy that formulates a system's control action as a solution to a constrained optimization problem. Utilizing a mathematical model of the system, MPC predicts and optimizes the system's future behavior through an iterative process, dynamically adjusting the control action based on the system's evolving state. The popularity of this approach stems from its ability to explicitly handle constraints, such as physical (e.g., flight speed and acceleration range of UAVs [45], [46], [47]) and environmental restrictions (e.g., no-fly zones [48], [49]). NMPC is a variant of MPC that can handle system non-linearity or its constraints. However, a real-time recursive solution to constrained optimization problems typically has high computational cost [50].

In multi-UAV systems, MPC has gradually been applied in various contexts, including obstacle-free environments, spatial environments with obstacles [48], and for generating collision-free trajectories for multiple drones [51]. Paper [48] discusses the application of MPC in leader-follower formation in obstacle-dense spaces. To achieve trajectory planning of wingmen, linear model-predictive control (LMPC) is used to control wingmen to maintain a constant distance from the virtual leader for formation control. In [47], MPC is employed to generate collision-free trajectories in real time for a group of UAVs in an environment with obstacles, where each drone has its own start and end point. The controller ensures that no collisions occur between drones during flight. NMPC is demonstrated to be capable of handling nonconvex collision problems in multi-UAV systems. MPC can also be combined with other collision avoidance strategies, such as the artificial potential

field method [43]. In [52], an NMPC is proposed that considers an LMPC to ensure collision-free paths between UAVs within formation but also combines the artificial potential field method. In [3], an NMPC is proposed that integrates the potential field method for trajectory planning in multi-UAV systems operating in obstacle-dense environments and verifies its effectiveness in a group of five drones.

In conclusion, the advantage of the NMPC scheme lies in its ability to generate collision-free trajectories for UAVs in obstacle-dense spaces, such as urban areas, collapsed buildings, or forests, while satisfying UAV dynamics, making the trajectories truly executable. In this particular application scenario, the main challenge with NMPC is the solution time. As the issue of solution time is addressed, control algorithms based on MPC and NMPC hold significant promise for multi-UAV swarm control in complex environments.

## C. Restricted Visual Field Model

Existing collective models predominantly assume that each particle can acquire global visual information [15], [16]. This global perspective provides individuals with the largest field of view and sufficient information, enabling the system to achieve the highest degree of cooperation. However, biological studies have demonstrated that the eyes of birds, such as starlings, pigeons, and owls, possess a limited field of view rather than a global perspective, with specific visual angles of  $143^\circ$ ,  $158^\circ$ , and  $100.5^\circ$ , respectively [17], [18], [53], [54]. Some studies have shown that flocks can attain better coordination patterns under optimal constrained vision than under global visibility.

Taking into account these observations, numerous researchers have conducted related studies to understand the biological mechanisms of collective models in nature [55], [56] and improve the convergence characteristics of such collective behavior [57], [58]. For instance, Lee and Ngo [59] investigated the effect of visual angle on the phase transition in a 2-D Vicsek model, finding that a phase transition occurs when the visual angle of each particle is greater than  $\pi/2$ . Furthermore, Li et al. [60] proposed a 3-D restricted visual field metric-free model, where each particle is governed by a restricted visual field. They demonstrated that the optimal viewing angle for each particle in the swarm increases with swarm size and stabilizes at  $155^\circ$ .

In vision-based UAV swarms, it is generally assumed that each individual can perceive the surrounding situation. Some researchers deploy monocular cameras at the front, back, left, and right sides of the UAVs, creating an omnidirectional view [19], [20]. Some researchers have studied UAVs with limited vision. Tian et al.'s [61] limited viewing angle model assumes that the boundaries of the limited potential field are symmetrically distributed on both sides of the individual's movement direction, meaning that the individual can only "look forward." Calvao and Brigatti [62] have recently introduced the concept of limited potential field range and gaze direction to model the ordered aggregation behavior of a group. In [63], they proposed a

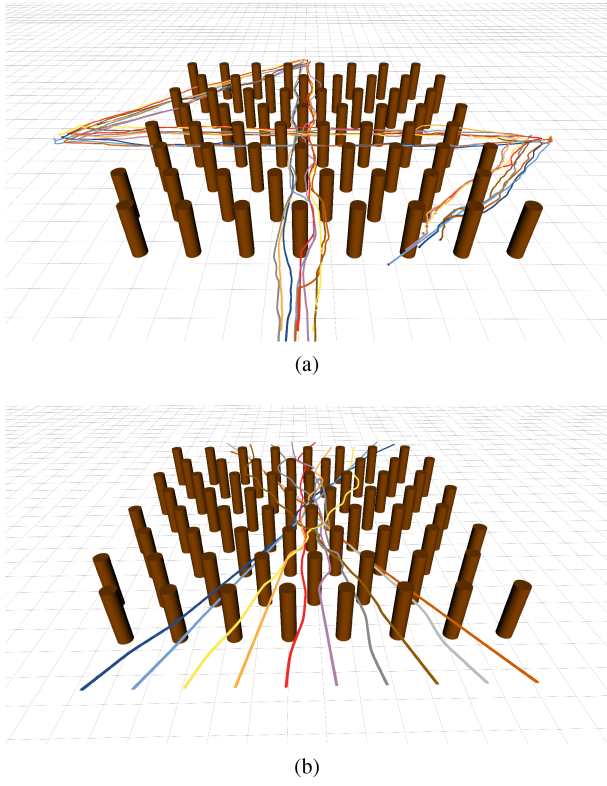


Fig. 1. Trajectory planning for multiple agents with limited vision employing the proposed method in a decentralized and asynchronous manner within an obstacle-dense environment. (a) Formation navigation through forest. (b) Intense reciprocal collision avoidance through forest.

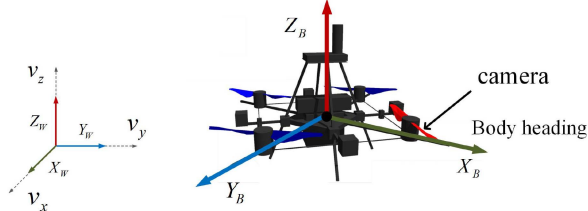


Fig. 2. Coordinate frames employed: representation of world ( $\mathbb{W}$ ) and body ( $\mathbb{B}$ ) coordinate systems in a control context.

group motion model with limited potential field angles and random LOS direction based on the basic Vicsek model. In the improved model, individuals can adjust their LOS direction to gather more information within a larger range.

### III. MODEL

We employ an NMPC framework for managing the flight of quadrotor UAVs (see Fig. 1). This framework amalgamates control, planning, and action objectives by utilizing numerical optimization techniques to compute trajectories adhering to the system dynamics constraints.

#### A. UAV Dynamic Equation

The coordinate systems of the UAV are illustrated in Fig. 2, where  $(X_B, Y_B, Z_B)$  denotes the body-fixed coordinate system, and  $(X_W, Y_W, Z_W)$  represents the global coordinate system [64]. Neglecting aerodynamics and motor dynamics,

the dynamics of a quadrotor drone can be modeled using the following equations:

$$\dot{p}_W = v_W \quad (1)$$

$$\dot{v}_W = g_W + q_W \odot c_B \quad (2)$$

$$\dot{q}_W = \frac{1}{2} \Lambda(\omega_B) \cdot q_W \quad (3)$$

$$\dot{\omega}_B = \mathbf{J}^{-1} (\eta - \omega_B \times \mathbf{J} \cdot \omega_B). \quad (4)$$

Here,  $p_W$ ,  $v_W$ , and  $q_W$  indicates the position, linear velocity, and attitude of the drone in the world coordinate system, respectively. The gravity vector  $g_W$  is expressed in the world frame. The term  $q_W \odot c_B$  denotes the rotation of the mass-normalized thrust vector  $c_B = (0, 0, c)^T$  by quaternion  $q_W$ .  $\Lambda(\omega_B)$  is a skew-symmetric matrix formed from the vector  $(0, \omega_B^T)^T = (0, w_x, w_y, w_z)^T$ , where  $\omega_B$  indicates the angular attitude velocity. The diagonal matrix  $J = \text{diag}(J_{xx}, J_{yy}, J_{zz})$  represents the quadrotor inertia, and  $\eta \in \mathbb{R}^3$  are the torques acting on the body due to the motor thrusts.

In the development of our NMPC control system, the controller is based on a simplified model of the quadrotor dynamics. This model is a streamlined version of the complete dynamics, where it specifically omits the dynamics associated with angular rates (4), focusing instead on (1)–(3) [65].

Within our NMPC framework, the state vector  $X$  and the control input vector  $u$  are organized as follows:  $X = [p_W, v_W, q_W]$ ,  $u = [c_B, \omega_B]$ , where  $p_W = [p_x, p_y, p_z]$  (abbreviated as  $p$ ) represents the position of the UAV in the world frame,  $v_W = [v_x, v_y, v_z]$  (abbreviated as  $v$ ) denotes its velocity, and  $q_W$  (abbreviated as  $q$ ) signifies the UAV's orientation. The control inputs include  $c_B$ , representing the mass-normalized thrust in the body frame of the UAV, and  $\omega_B$ , which corresponds to the angular velocity essential for controlling the UAV's orientation.

In summary, the dynamics of the UAV within the MPC control system are succinctly expressed by the following equation:

$$X(t+1) = \zeta(X(t), u(t)). \quad (5)$$

This representation effectively captures the essential aspects of UAV dynamics pertinent to our control objectives in the NMPC framework.

The time interval  $T_h$  is divided into discrete time steps  $dt$ , with state and control discretized as  $X(\cdot | t) = \{X(k+t | t) \forall k \in [1, N+1]\}$  and  $u(\cdot | t) = \{u(k+t | t) \forall k \in [1, N-1]\}$ . Let  $X(k+t)$  denote the predicted state at time step  $k+t$ , produced at the time step  $t$ . The corresponding control actions are denoted by  $u(k+t)$ .  $X(\cdot | t) \in \mathbb{R}^{10N}$  is the superposition sequence of predicted states  $X(k+t | t)$  in prediction time periods  $k \in \{1, \dots, N\}$  produced at the time step  $t$ , while  $u(\cdot | t) \in \mathbb{R}^{4N}$  is the superposition sequence of predicted control inputs  $u(k+t | t)$  in prediction time periods  $k \in \{1, \dots, N-1\}$  produced at the time step  $t$ .

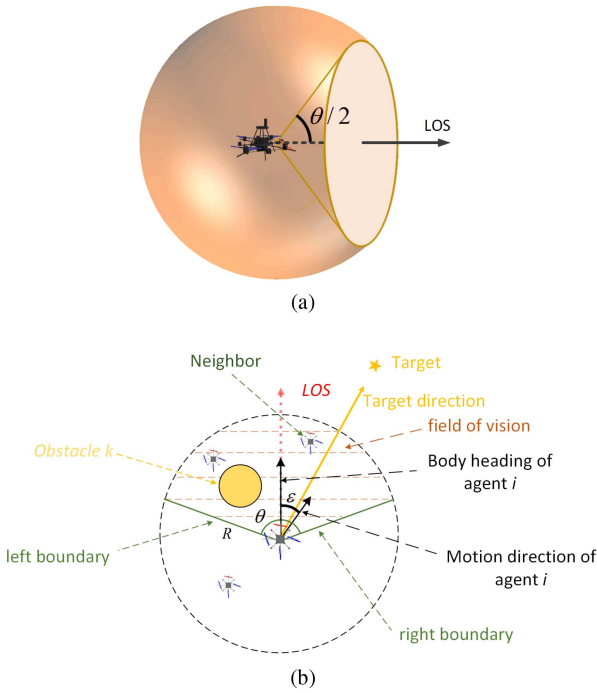


Fig. 3. Restricted visual field model based on random LOS demonstrated in 3-D and 2-D. (a) 3-D schematic diagram. (b) 2-D schematic diagram.

### B. Restricted Visual Field Model Based on Random LOS

In this article, we adopt a limited-field-of-view model with a random LOS to define the drone's perceptual capabilities and range concerning obstacles and neighboring drones in the environment.

As illustrated in Fig. 3, the field of view for a single drone is a sector area bounded by  $\phi$  and  $R$ , with the drone situated at the sector's center and the symmetry axis pointing toward its forward direction, also referred to as the LOS. The left and right boundaries of the field of view form an angle  $\theta/2$  with the forward direction. During flight, drones can acquire state information of neighboring drones entering their field of view through an onboard camera, including relative position and velocity. Drones can detect and identify neighboring drones using object detection algorithms, such as YOLO-v7 [66], and subsequently estimate their relative position and velocity by employing multiagent localization and tracking techniques [19].

As shown in Fig. 3,  $\text{FOV}_i(L_i(t), \phi)$  is the visual field of agent  $i$  at moment  $t$ .  $\mathcal{N}_i(t)$  is the neighbor set of agent  $i$  at moment  $t$ . Neighbors need to be within the drone's visual field and not obscured by obstacles

$$\begin{aligned} \mathcal{N}_i(t) &= \left\{ j \mid p_j(t) \in \text{FOV}_i(L_i(t), \phi), j = 1, \dots, N \right\} \\ &= \left\{ j \mid \|p_j(t) - p_i(t)\| \leq R \wedge \langle (p_{ij}(t), L_i(t)) \rangle \leq \frac{\omega}{2} \right. \\ &\quad \left. \wedge f(p_{ij}(t) - O_l) < 0, j = 1, \dots, N \right\} \end{aligned} \quad (6)$$

in which  $p_{ij}(t)$  is the vector pointing from agent  $i$  to  $j$  at moment  $t$ .  $L_i(t)$  is the LOS of the drone.  $\langle p_{ij}(t), L_i(t) \rangle$  is the

clamping angle of the two vectors.  $d_{ij}^2(t)$  is the Euclidean distance between agent  $i$  and  $j$ , and  $f(p_{ij}(t) - O_l)$  defines that the line segment from agent  $i$  to  $j$  does not intersect the obstacle  $O_l$ .

During the flight of the UAV, the direction of the UAV's LOS is generally related to the direction of motion. Consequently, neighboring agents may not be entirely visible to the host drone. However, by adjusting the LOS, agents outside the current visual field may become visible in the next moment. To expand the field of view, drones can oscillate, ensuring focus on the front while dynamically enlarging the side views. This approach increases the probability of neighboring agents entering the focal individual's potential field from all directions. To further enhance the probability of side neighbors entering the drone's field of view, a random factor  $\varepsilon$  is incorporated into the sightline direction, which follows a normal distribution  $N(\mu, \sigma^2)$

$$L_i(t) = \tan^{-1} \left( \frac{v_y}{v_x} \right) + \varepsilon. \quad (7)$$

### C. Critical Node Selection for Neighbor Aircraft

The Boids model and the Vicsek model demonstrate that local interactions among agents are sufficient to produce collective behavior of group animals [67]. Ballerini et al. [68] argue that this interaction is based on a topological rather than a metric pattern. Experimental data reveal that an important topological characteristic of bird interaction is the limited number of neighbors (six or seven at most) with which each individual interacts.

The airspace composed of drones is called a collision airspace. A directed graph  $\mathcal{G} = (\mathcal{V}, \mathcal{E})$  is used to model the drone swarm, where the vertex set  $\mathcal{V} = \{1, \dots, N\}$  represents the drones and the edge set  $\mathcal{E} \subseteq \mathcal{V} \times \mathcal{V}$  contains pairs of drones  $(i, j) \in \mathcal{E}$ , indicating that drone  $j$  is within the field of view of drone  $i$  according to Section III-B.

We model all UAVs involved in conflicts as network nodes and connect them with edges. Each edge has an attribute representing the mutual threat level between two agents, depending on the relative distance and approach speed of the UAVs. The attribute of each edge, denoted as  $R_{ij}$ , represents the level of threat between two drones  $i$  and  $j$

$$R_{ij} = \frac{\text{RD}_{ij}}{\text{RS}_{ij}} \quad (8)$$

$$\text{RD}_{ij} = e^{\|p_{ij}\| - d_{\text{ref}}} \quad (9)$$

$$\text{RS}_{ij} = \frac{p_{ij} \times (v_i - v_j)}{\|p_{ij}\|}. \quad (10)$$

$\text{RD}_{ij}$  calculate the relative distance between two objects,  $i$  and  $j$ , based on their respective position vector  $p_{ij}$  and reference distance  $d_{\text{ref}}$ . The exponential function serves to highlight the difference between the actual distance and the reference distance, making the relative distance more sensitive to changes as the actual distance deviates from the reference distance.

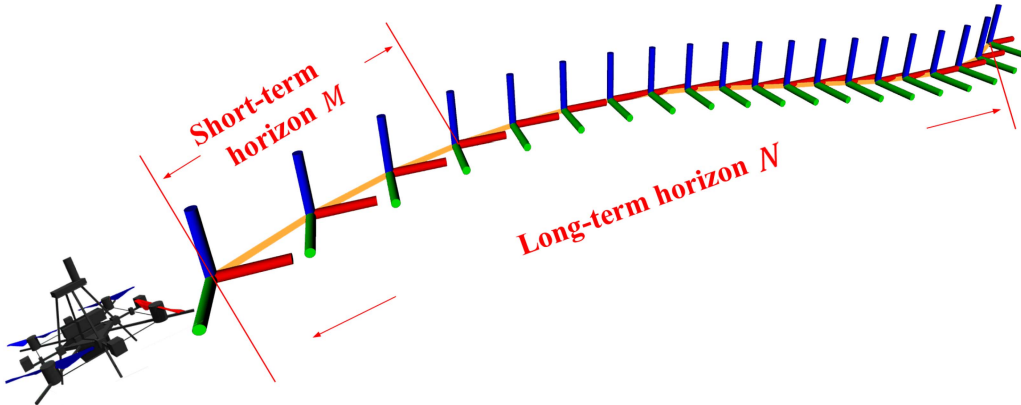


Fig. 4. Predicted trajectory based on the proposed dual-horizon NMPC.

$RS_{ij}$  calculates the approaching speed of two objects,  $i$  and  $j$ .  $v_{ij}$  represents the relative velocity vector.  $\|p_{ij}\|$  represents the norm of relative position. The dot product  $p_{ij} \cdot v_{ij}$  calculates the component of the relative velocity vector that lies along the direction of the position vector  $p_{ij}$ .

To reduce the network complexity, improve the computation speed, lower the system latency, and enhance the UAVs' reaction speed in the network, we limit the out-degree of each node to less than 4, i.e., for each UAV, only the three most threatening UAVs among all conflicting ones are selected. Based on this, we construct a dynamic complex network of UAVs, where nodes represent UAVs with threat relationships and edges represent threat relationships with attributes indicating threat levels.

In this dynamic complex network, the objective is to mitigate potential conflicts and maintain safe distances between UAVs while achieving cooperative goals. By limiting the out-degree of each node to less than 4, the computational burden is reduced, enabling faster decision making and improved responsiveness for the UAVs.

#### D. Cost Function and Constraints

The UAVs' system dynamics are discretized using a sampling time of  $T_s$ . The resulting discrete model serves as the prediction model for the MPC. Predictions are executed with a receding horizon, taking a specified number of future steps into consideration. This prediction horizon is denoted as the NMPC horizon. Innovatively, we establish two distinct prediction horizons in this article: long- and short-term horizons,  $N$  and  $M$ . By attributing a cost to a state and input configuration at both the current time and within the prediction, a nonlinear optimizer is employed to identify the optimal set of control actions, as defined by the minimum cost of the cost function. Within the MPC framework, an open-loop control problem is continuously optimized, and the initial control command from the optimal prediction sequence is applied.

In the MPC control model, future control commands for UAVs are planned through objective and constraint terms. As shown in Fig. 4, the cost function comprises three components: short-term reactive action, long-term planning

action, and control effort. Specifically, short-term reactive action involves rapidly responding to perceived external disturbances to maintain stable flight, akin to the behavioral mechanism of insects. Long-term planning action is focused on devising comprehensive collision-free trajectories to enhance flight efficiency and safety, which also mirrors the behavioral mechanism of insects. Finally, the control effort aims to minimize the agents' accelerations, thereby smoothing flight trajectories, increasing energy efficiency, and penalizing changes in successive inputs. Thus, we formulate the cost functions as

$$\begin{aligned} J(X(\cdot | t), u(\cdot | t)) = & \sum_{k=1}^M \text{Short}(X(k+t | t)) \\ & + \sum_{k=1}^N \text{Long}(X(k+t | t)) \\ & + \sum_{k=1}^{N-1} \text{Control}(u(k+t | t)). \end{aligned} \quad (11)$$

$\sum_{k=1}^M \text{Short}(X(k+t | t))$  is the cost for short-term reactive action,  $\sum_{k=1}^N \text{Long}(X(k+t | t))$  is the cost for long-term planning action, and  $\sum_{k=1}^{N-1} \text{Control}(u(k+t | t))$  is the cost for the control term.  $r(x, u) = 0$  is the equation constraint imposed by system dynamics.  $h(x, u) \leq 0$  is an optional boundary for control and state quantities.

1) *Short-Term Reactive Action:* In the dynamic swarm motion of UAVs, the drones' state is constantly changing. As UAVs rely on onboard cameras and computational vision to obtain the current state information of neighboring agents, including relative position and velocity, accurately predicting the future state of neighbors is challenging. Consequently, real-time active control is necessary to prevent collisions between individuals while maintaining the swarm aggregation. For this purpose, a short-term reactive action term is constructed in the MPC objective function to prevent collisions among neighboring UAVs and maintain an appropriate interagent distance and formation shapes.

Drawing from Reynolds' model in swarm intelligence literature, this term incorporates both aggregation and repulsion components to maintain an optimal distance  $d_{\text{ref}}$  from neighboring UAVs. The short-term reactive action of drone  $i$  at time instant  $t + k$  is defined as follows:

$$\text{Short}(X(k+t|t)) = \sum_{j \in \mathcal{N}_i} \frac{w_{\text{short}}}{N_i} (\|p_j(k+t|t) - p_i(k+t|t)\|^2 - d_{\text{ref}}^2). \quad (12)$$

$\mathcal{N}_i$  is the neighbor set of drone  $i$ , that is, a collection of drones in the field of view of drone  $i$  according to Section III-B.  $p_j(k+t|t)$  is the estimated position of neighboring agent  $j$  at moment  $k+t$ , produced at the time moment  $t$ , by drone  $i$ . Speed estimation information of neighboring agent  $j$  is  $v_j(t|t)$ .

$$p_j(t|t) = p_j(t) \quad (13)$$

$$p_j(k+t|t) = p_j(t|t) + v_j(t|t) * k * dt. \quad (14)$$

To prevent inner collision with neighboring agents, short-term constraints are added to the inequality constraints

$$h_{\text{short}}(X, u) \leq 0 \quad (15)$$

$$h_{\text{short}}(X, u) = d_{\text{agent-safety}} - \|p_j(k+t|t) - p_i(k+t|t)\| \quad \forall j \in \mathcal{N}_i \forall k \in \{0, 1, \dots, M\} \quad (16)$$

where  $d_{\text{agent-safety}}$  is the safe distance between two drones.

2) *Long-Term Planning Action*: To regulate a drone's motion toward a target while avoiding spatial obstacles, we incorporate a long-term planning action term into the MPC objective function. This term considers the positions of the target and obstacles, which are assumed to remain fixed during the UAV's motion. The long-term planning action of the UAV at each time step is formulated as follows:

$$\text{Long}(X(k+t|t)) = w_{\text{mig}}(\|v_i(k+t|t) - \text{ref}(k+t|t)\|) \quad (17)$$

$$\text{ref}(k+t|t) = \mathbb{C} \frac{\text{goal} - p_i(k+t|t)}{\|\text{goal} - p_i(k+t|t)\|}. \quad (18)$$

The migration term integrates the effects of direction and velocity magnitude, enabling the drone to move toward the target point at the desired speed magnitude  $\mathbb{C}$ . The velocity direction only encodes the long-term goal of the drone, without considering a collision-free path.

To prevent collisions with obstacles, a long-term constraint is added to the inequality constraints  $h(X, u) \leq 0$ . This approach effectively balances target navigation and obstacle avoidance, facilitating safe and efficient UAV motion

$$h_{\text{long}}(X, u) \leq 0 \quad (19)$$

$$h_{\text{long}}(X, u) = d_{\text{obstacle-safety}} - \|p_l^{\text{obs}} - p(k+t|t)\| \quad \forall l \in O_i \forall k \in \{0, 1, \dots, N\}. \quad (20)$$

$O_i$  is the set of obstacles near agent  $i$ , and  $p_l^{\text{obs}}$  is the position of obstacle  $l$ .

3) *Control Objective Term*: The control effort within our NMPC framework aims to smooth the UAV's flight trajectories and enhance energy efficiency by minimizing abrupt changes in successive inputs. The control effort term is formulated as follows:

$$\begin{aligned} \text{Control}(u(k+t)) = \\ = w_{c1} \|c_B(k+t|t) - c_B(k+t-1|t)\| \\ + w_{c2} \|\omega_B(k+t|t) - \omega_B(k+t-1|t)\| \\ + w_{c3} \|c_B(k+t|t)\| + w_{c4} \|\omega_B(k+t|t)\|. \end{aligned} \quad (21)$$

The combination of these terms in the control function aims to achieve a balance between maintaining smooth flight (by minimizing abrupt changes in thrust and angular velocity) and conserving energy (by penalizing excessive thrust and rotational speed). By adjusting the weights  $w_{c1}$ ,  $w_{c2}$ ,  $w_{c3}$ , and  $w_{c4}$ , the control strategy can be fine-tuned to prioritize either smoothness or energy efficiency.

To prevent aggressive or oscillatory behavior in control inputs, we integrate a controlling-term constraint into the inequality constraints  $h(X, u) \leq 0$ . This constraint is designed to impose restrictions on the successive differences of control actions and establish a limit on the magnitude of change in control inputs

$$c_B(k+t+1|t) - c_B(k+t|t) < \Delta c_{\max} \quad (22)$$

$$\omega_B(k+t+1|t) - \omega_B(k+t|t) < \Delta \omega_{\max}. \quad (23)$$

This constraint ensures that the change in control inputs between consecutive time steps does not exceed the thresholds  $\Delta c_{\max}$  and  $\Delta \omega_{\max}$ , promoting consistent and gradual maneuvering.

In our NMPC framework, direct constraints on the control inputs are applied, considering the real-world operational limits of a UAV. These constraints are crucial for ensuring that the low-level controller can effectively stabilize the UAV's attitude within a practical range. The constraints on the control inputs are defined as

$$c_{\min} \leq \|c_B(k+t|t)\| \leq c_{\max} \quad (24)$$

$$\omega_{\min} \leq \|\omega_B(k+t|t)\| \leq \omega_{\max}. \quad (25)$$

Here,  $c_{\min}$  and  $c_{\max}$  represent the minimum and maximum bounds for the mass-normalized thrust vector  $c_B$ , respectively, while  $\omega_{\min}$  and  $\omega_{\max}$  represent the minimum and maximum bounds for the angular velocity  $\omega_B$ , respectively.

## E. Optimization

The NMPC problem is solved by CasADi [69], which employs the following formulation for a nonlinear program (NLP)

$$\min_{z, p} f(z, p) \quad (26)$$

subject to

$$\underline{z} \leq z \leq \bar{z}, \quad p = \underline{p}, \quad \underline{g} \leq g(z, p) \leq \bar{g}.$$

This parametric NLP features an objective function  $f(z, p)$  and a constraint function  $g(z, p)$  that depend on the decision variable  $z$  and a known parameter  $p$ . For equality

constraints, the variable bounds  $[\underline{z}, \bar{z}]$  or constraint bounds  $[g, \bar{g}]$  are equal. The proposed NMPC controller fits into the NLP by performing a multishooting of the cost function via a decision variable  $z = [X(\cdot | t), u(\cdot | t)]$ , defining  $z$  based on the input constraints. We also define  $F$  to cast the equality constraints. The parameter  $p$  is set to encompass initial conditions  $X(0)$ , neighbor states, goal point, and the obstacles.

Considering the constraints, the solution of (26) yields a primal  $(z, p)$  and a dual  $(\lambda_z, \lambda_p, \lambda_g)$  solution, where the Lagrange multipliers are selected to be consistent with the following definition of the Lagrangian function:

$$\mathcal{L}(z, p, \lambda_z, \lambda_p, \lambda_g) := f(z, p) + \lambda_z^\top z + \lambda_p^\top p + \lambda_g^\top g(z, p) \quad (27)$$

where  $\lambda_p$  is the parametric sensitivity of the object with respect to the parameter vector  $p$ .

Based on the cost function and constraints outlined in Section III-D, we can formulate the NMPC problem as

$$\pi^*(t) = \min_{X, u} J(X, u, p) \quad (28)$$

$$\begin{aligned} \pi^*(t) = & \min_{X, u} \sum_{k=0}^M \sum_{j \in \mathcal{N}_i} \frac{w_{\text{short}}}{N_i} (\|p_j(k+t | t) - p_i(k+t | t)\| - d_{\text{ref}})^2 \\ & + \sum_{k=0}^N w_{\text{mig}} \|v_i(k+t | t) - \text{ref}(k+t | t)\| \\ & + \sum_{k=0}^{N-1} (w_{c1} \|c_B(k+t | t) - c_B(k+t-1 | t)\| \\ & + w_{c2} \|\omega_B(k+t | t) - \omega_B(k+t-1 | t)\| \\ & + w_{c3} \|c_B(k+t | t)\| + w_{c4} \|\omega_B(k+t | t)\|) \end{aligned} \quad (29)$$

subject to

$$X(t | t) = X(t) \quad \forall k \in \{0, \dots, N-1\} \quad (30)$$

$$X(t+k+1 | t) = \zeta(X(t+k | t), u(t+k | t)) \quad (31)$$

$$\forall k \in \{1, \dots, N-1\} \quad (31)$$

$$v_{\min} \leq \|v(k+t | t)\| \leq v_{\max} \quad (32)$$

$$\|c_B(k+t+1 | t) - c_B(k+t | t)\| < \Delta c_{\max} \quad (33)$$

$$\|\omega_B(k+t+1 | t) - \omega_B(k+t | t)\| < \Delta \omega_{\max} \quad (34)$$

$$c_{\min} \leq \|c_B(k+t | t)\| \leq c_{\max} \quad (35)$$

$$\omega_{\min} \leq \|\omega_B(k+t | t)\| \leq \omega_{\max} \quad (36)$$

$$d_{ij}(k+t | t)^2 \geq d_{\text{agent-safety}}^2 \quad (37)$$

$$d_{il}(k+t | t)^2 \geq d_{\text{obs-safety}}^2 \quad (38)$$

$$k \in \{1, \dots, N-1\}, j \in \mathcal{N}_i, \text{ and } \forall l \in O_i.$$

The proposed NMPC controller operates at a sampling frequency of 10 Hz and a prediction horizon of 2 s, divided into 20 intervals of 0.1 s. The prediction horizon includes a short-term horizon (0.5 s) and a long-term horizon (2 s).

This design ensures efficient and accurate control, adapting swiftly to changes in system dynamics and effectively managing system constraints.

#### IV. NUMERICAL SIMULATION

We developed multiple simulation environments within the ROS-Gazebo framework to validate our model for controlling a formation of multi-UAVs.

The ROS-Gazebo framework is a robust and flexible platform for simulating robotic systems, including sensors, controllers, and actuators. Each UAV's state estimation and control are performed using the Gazebo simulator and the Betaflight controller. Communication between nodes is established using the ROS, and we executed the simulations in Gazebo while displaying the trajectory in Rviz, a visualization tool commonly employed in robotics research for presenting 3-D data. In simulation experiments, we demonstrated three challenging applications that validated various aspects of performance and potential of our system solution. Moreover, we conducted quantitative evaluations of several common metrics for each application.

##### A. Scenario 1: Formation Navigation Through Forest

Fig. 5 illustrates the simulation environment constructed in Gazebo, which simulates a forest environment populated with cylindrical obstacles [see Fig. 5(a)]. The positions of the obstacles on the map are random but uniformly distributed, with a radius of 1 m and a spacing of 7 m between each cylinder. The total occupied area of the environment is approximately 50 m × 50 m. The swarm consists of nine drones, initially arranged in an ordered formation located in front of the forest [see Fig. 5(b)] with a lateral and longitudinal spacing of 1.5 m [see Fig. 5(c)]. During the experiment, the swarm is required to sequentially reach three target points and return to the starting point while avoiding the obstacles and maintaining an appropriate formation to prevent dispersion [as shown in Fig. 5(d)].

Fig. 6 provides a 3-D visualization of the UAV flight process in Rviz. Fig. 6(a) displays the 3-D trajectory of the UAV swarm, which sequentially navigates through three target points while avoiding obstacles and maintaining a cohesive formation [see Fig. 6(b)]. During the flight, at each moment, the UAVs assess the threat level with neighboring UAVs based on their state and construct a complex network [see Fig. 6(c)]. Subsequently, the proposed MPC controller generates a predicted trajectory, as presented in Fig. 6(d), and the first control signal of the predicted sequence is then fed into the autopilot to control the UAV flight.

Fig. 7 presents the simulation results of UAVs crossing the forest under the NMPC controller. The UAVs are able to navigate the forest in a formation and reach the designated target points. Throughout the entire process, the distance between the UAVs during flight consistently remains above the safety threshold, as shown in Fig. 7(b), and no collisions occur. All UAVs successfully avoid collisions with obstacles, as the distance between them and the obstacles consistently remains above the safety threshold, as shown

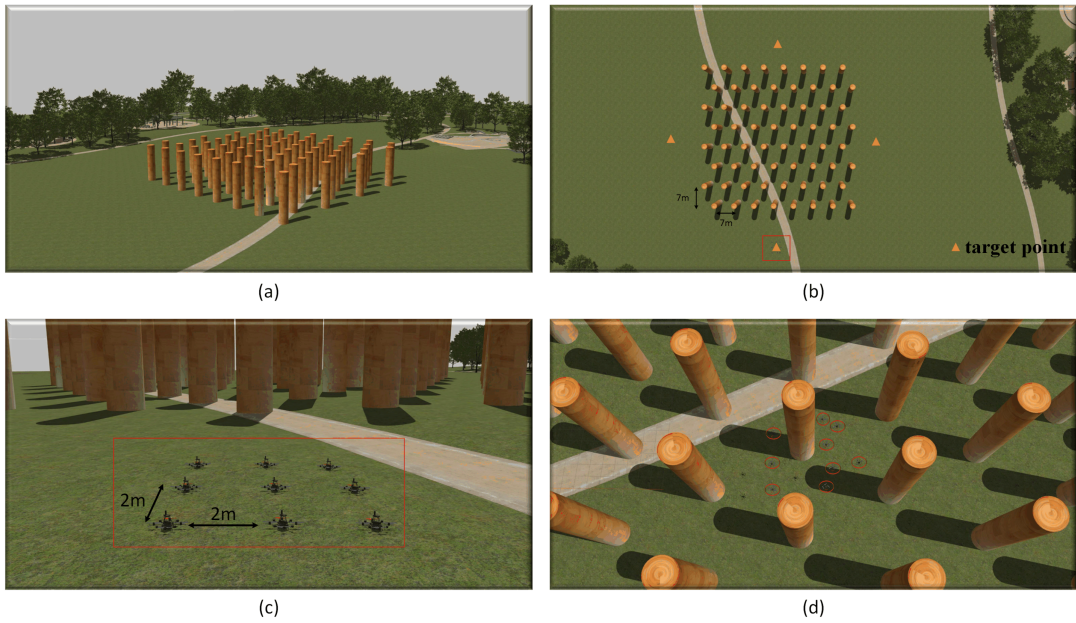


Fig. 5. Gazebo simulation environment. (a) Front view of the Gazebo simulation environment, with 49 uniformly distributed cylinders with a radius of 1 m, occupying an area of approximately  $(50 \text{ m} \times 50 \text{ m})$ . (b) Top view of the Gazebo simulation environment, including three target points (marked by triangles). The UAVs sequentially navigate through the targets while flying through a forest filled with cylindrical obstacles. (c) Formation arrangement of the drones before taking off. (d) Flight of the drone formation in the forest while maintaining an appropriate formation and avoiding the obstacles.

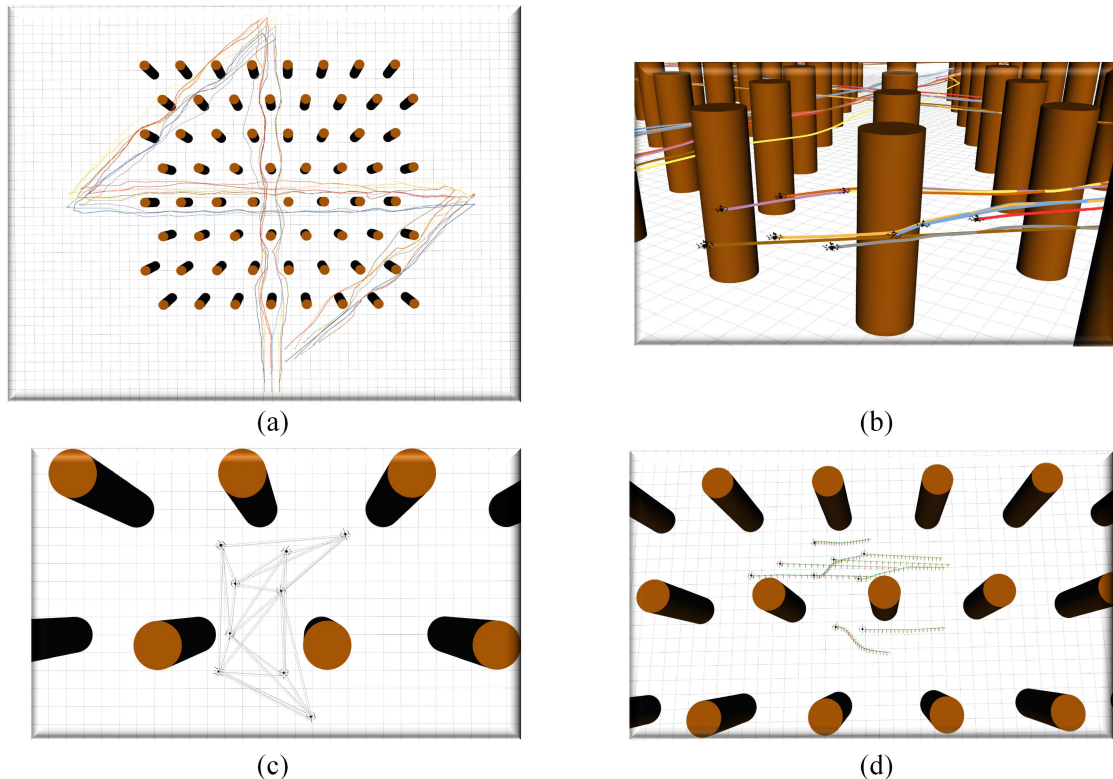


Fig. 6. Demonstration in Rviz. (a) 3-D trajectory map of multi-UAVs in Rviz. (b) Cooperative flight map of multiple UAVs, avoiding obstacles while maintaining a cohesive formation. (c) Complex network diagram constructed by multiple UAVs during flight based on threat assessment. (d) Planned trajectory generated by the proposed MPC controller during UAV flight.

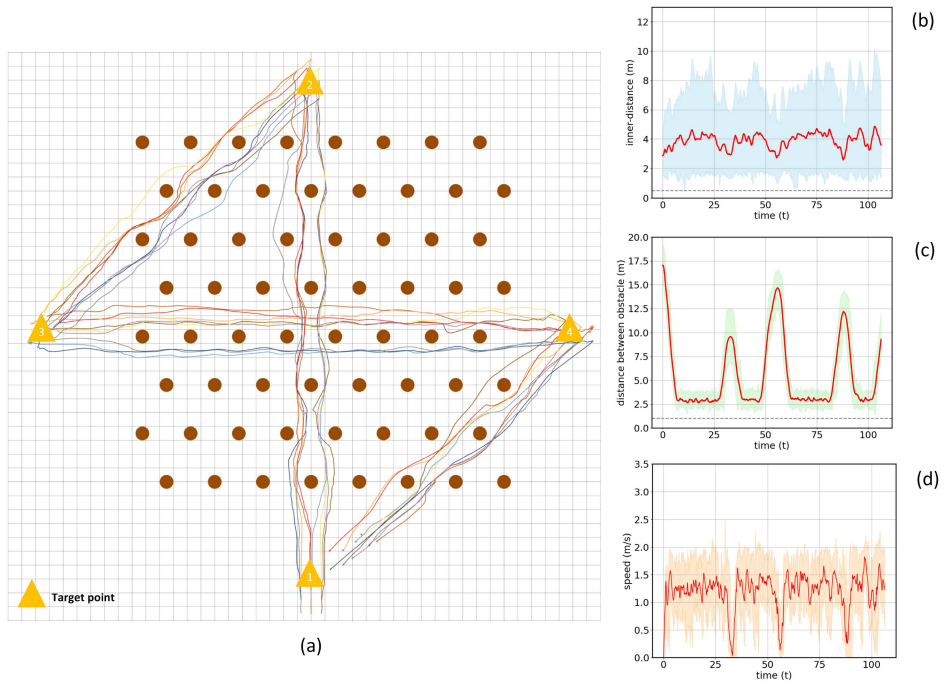


Fig. 7. Simulation and analysis of formation flight crossing the forest using NMPC controller. (a) 2-D trajectory of nine UAVs flying in formation. (b) Mean inner distance (solid line) and standard deviation (shaded area) between UAVs. (c) Mean distance (solid line) and standard deviation (shaded area) between UAVs and nearest obstacles. (d) Mean speed (solid line) and standard deviation (shaded area) of UAVs.

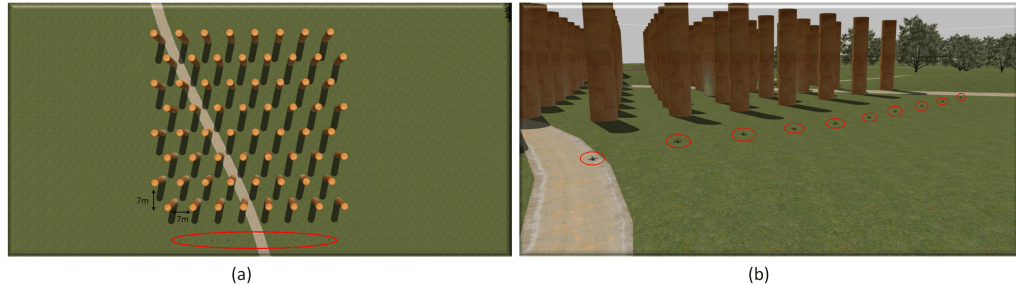


Fig. 8. Gazebo simulation environment. (a) Top view of gazebo simulation environment, filled with 49 columns of 1-m radius. (b) Formation arrangement of the drones before taking off.

in Fig. 7(c). The average speed of multiple UAVs is 1.5 m/s, as shown in Fig. 7(d).

The simulation results show that the multi-UAVs can maintain their swarm formation. They deviate slightly from their trajectories when they encounter obstacles and then resume their original speed and direction after avoiding them. The formation speed varies inversely with the obstacle density, reflecting a tradeoff between safety and flight time. The speed changes of some individuals propagate through the whole formation, indicating a collective response to environmental challenges and the emergence of group order among independent individuals.

#### B. Scenario 2: Intense Reciprocal Collision Avoidance Through Forest

Scenario 2, similar to Scenario 1, simulates a forest environment with cylindrical obstacles (see Fig. 8). However, unlike Scenario 1, where the UAVs move in a similar

direction and maintain a formation, with limited apparent avoidance behavior between them. The UAVs in Scenario 2 are assigned distinct target points, and their trajectories intersect in a confined space, emphasizing the utmost importance of collision avoidance among the UAVs. This scenario mimics the most fundamental requirements of dense air traffic: safe, efficient, distributed, and asynchronous navigation.

Fig. 9 presents a 3-D visualization of the UAV flight process based on Rviz. In Fig. 9(a), the 3-D trajectory of the UAV formation is displayed, demonstrating that the formation successfully reaches the target point while avoiding obstacles. Multiple UAVs converge in the red area, and the UAVs need to fly carefully to avoid collisions. In Fig. 9(b), the UAVs generate predicted trajectories based on the MPC controller, which considers obstacle avoidance. The first control signal of the predicted sequence is then input into the autopilot system. The results suggest that the proposed

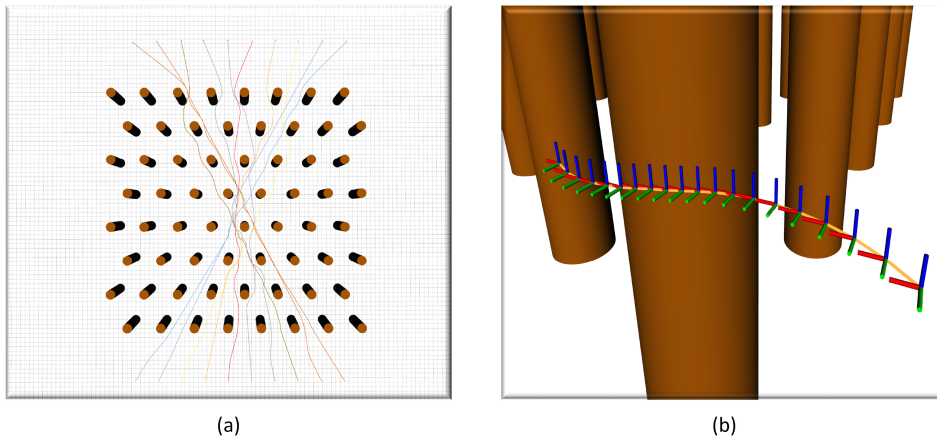


Fig. 9. (a) 3-D trajectory of multiple UAVs. (b) Predicted trajectory of UAVs during flight.

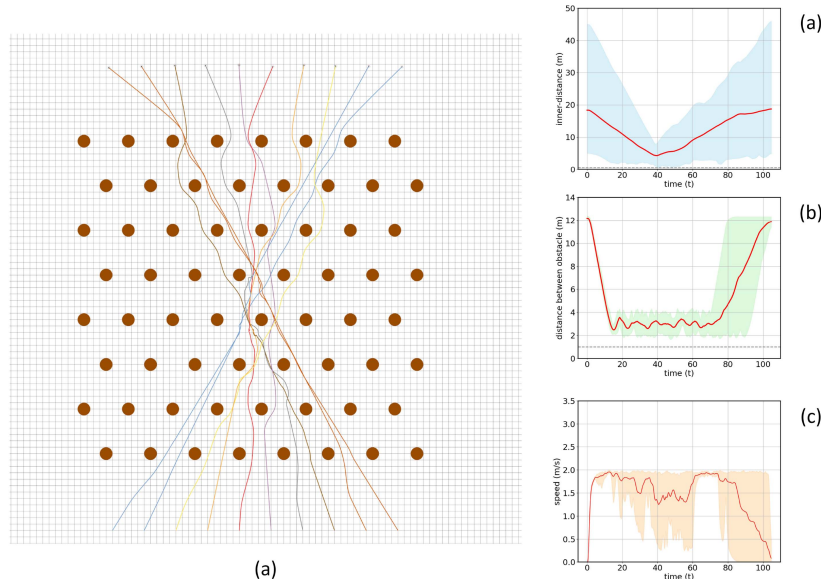


Fig. 10. Simulation and analysis of intensive reciprocal avoidance of multi-UAV using the NMPC controller. (a) 2-D trajectory of ten UAVs flying independently and autonomously. (b) Mean inner distance (solid line) and standard deviation (shaded area) between UAVs. (c) Mean distance (solid line) and standard deviation (shaded area) between UAVs and nearest obstacles. (d) Mean speed (solid line) and standard deviation (shaded area) of UAVs.

MPC controller is effective in generating safe and efficient trajectories for UAVs in complex environments.

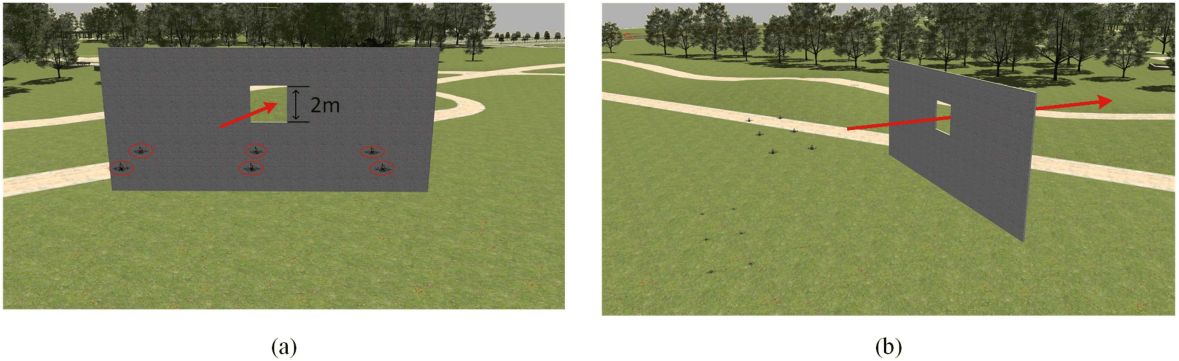
Fig. 10 presents the simulation results of UAVs crossing the forest under the NMPC controller. The UAVs are able to cross the forest and reach their designated target points without any internal collisions occurring among them. Throughout the flight, the distance between agents is always kept above the safety threshold [see Fig. 10(b)]. All UAVs successfully avoid collisions with obstacles, and the distance between UAVs and obstacles is always kept above the safety threshold [see Fig. 10(c)]. The average speed of multiple UAVs was 1.5 m/s [see Fig. 10(d)].

Despite encountering unpredictable events, the UAVs in the simulation are able to maintain a safe distance from obstacles and other drones. The velocity profile indicates that when multiple drones converge in crowded areas filled

with obstacles, the drones' speeds significantly decrease to ensure safety. After passing through the congested areas, the drones gradually resume their speed. This demonstrates the adaptability and effectiveness of the proposed MPC controller in managing complex scenarios, emphasizing its potential for real-world applications in dense air traffic environments.

### C. Scenario 3: Formation Crossing the Hole

In the third scenario, the simulation takes place in an urban environment where the drone swarm is required to fly through a tunnel, as shown in Fig. 11(a) and (b). At the beginning of the experiment, the six drones hover in front of the tunnel entrance, and then, a migration direction is given to the swarm. The drones autonomously make decisions based on fully distributed, limited vision to fly through the



(a)

(b)

Fig. 11. (a) and (b) Gazebo simulation environment; the drone formation is required to pass through a tunnel of a certain size ( $2 \text{ m} \times 2 \text{ m}$ ). The formation is given a forward migration direction and tasked with autonomously making decisions in a fully distributed and limited visual environment to pass through the tunnel.

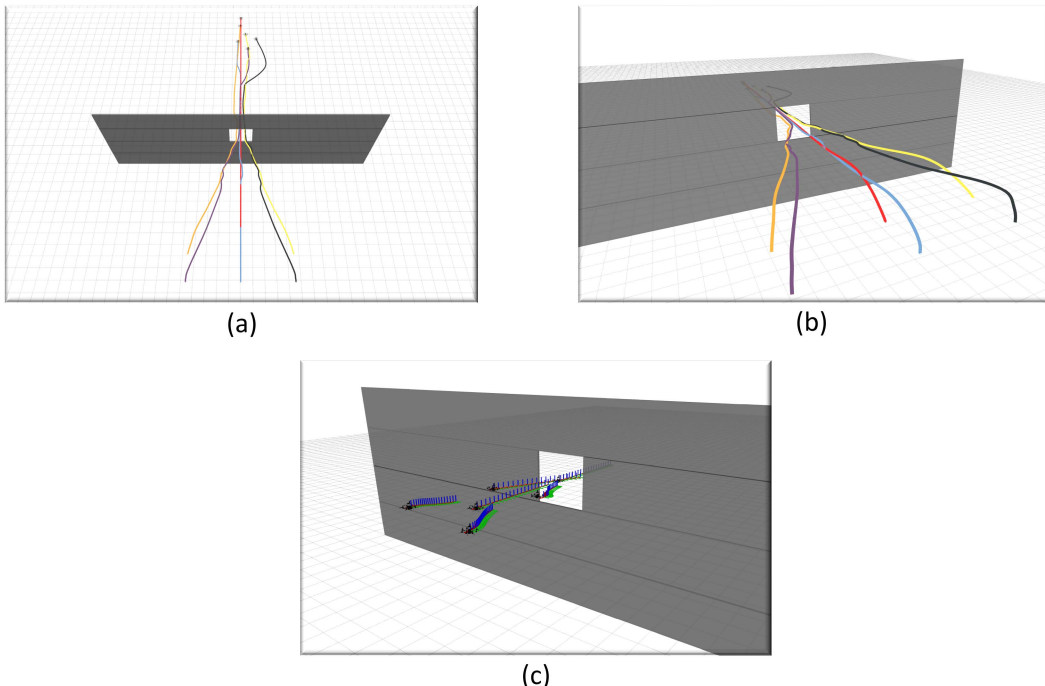


Fig. 12. Demonstration of the motion process in Rviz. (a) and (b) 3-D trajectory map of multi-UAVs. (c) Planned trajectory generated by the proposed MPC controller during UAV flight when crossing the hole.

tunnel. During the swarm flight, the drones need to avoid collisions with the tunnel walls, maintain swarm cohesion, and prevent collisions.

Fig. 12 showcases a 3-D visualization of the drone flight process based on Rviz. As the drone formation approaches the vicinity of the aperture in the simulated city environment, it decelerates and hovers before proceeding to pass through the opening sequentially. During the formation flight, the drones are required to avoid collisions with the walls while maintaining cohesion and preventing collisions with one another, all within a limited field of view.

The simulation results of UAV passage through the tunnel under the distributed NMPC controller are presented in Fig. 13. The UAV formation is able to autonomously pass through the tunnel and reach the target point without

any internal collisions during the entire process. The interdrone distance is always above the safety threshold [see Fig. 13(b)], and all UAVs successfully avoid collision with the walls, maintaining a safe distance from the obstacles [see Fig. 13(c)]. The average speed of multiple UAVs during the experiment is 1.5 m/s [see Fig. 13(d)].

These results demonstrate the successful passage of the UAV formation through the tunnel, maintaining a safe distance between the drones and avoiding collisions. The reduction in UAV speed when passing through congested areas ensures safety. The experiment provides compelling evidence for the outstanding performance of the distributed NMPC controller in limited visual range and complex environments, highlighting the great potential of distributed UAV formations in practical applications.

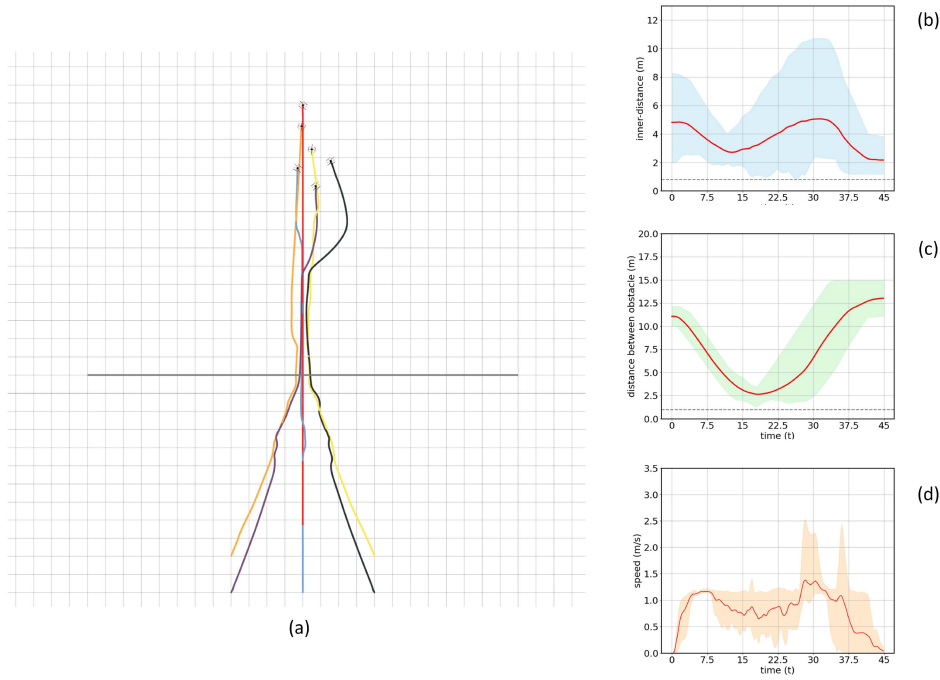


Fig. 13. Simulation and analysis of formation flight through a hole using the NMPC controller. (a) 2-D trajectory of five UAVs flying in formation. (b) Mean inner distance (solid line) and standard deviation (shaded area) between UAVs. (c) Mean distance (solid line) and standard deviation (shaded area) between UAVs and nearest obstacles. (d) Mean speed (solid line) and standard deviation (shaded area) of UAVs.

## V. CONCLUSION

This article presents a dual-horizon NMPC scheme for vision-limited multi-UAV systems, addressing the challenges of autonomous cooperative flight in complex and unknown scenarios. The online optimization problem is solved at a frequency at 10 Hz without violation of the established obstacle or input constraints.

The proposed approach introduces two key innovations: a restricted visual field with a random LOS model and a dual-horizon NMPC controller. This combination enables distributed cooperative flight, obstacle avoidance, and navigation, providing real-time solutions suitable for local path planning.

The main contributions of this work include the consideration of a more realistic restricted visual field, the design of a dual-horizon NMPC controller that efficiently adapts to changing situations, and the implementation of a fully distributed and asynchronous system, which allows for cooperative goal achievement. In addition, our approach models UAV dynamics using ROS and Betaflight, validating the effectiveness of our algorithms through challenging simulation scenarios in Gazebo.

The presented dual-horizon NMPC scheme offers promising results in handling simulated scenarios, demonstrating its potential for practical applications in multi-UAV swarm control within complex environments. Future work may focus on further enhancing the efficiency and robustness of the proposed approach, as well as exploring scenarios to validate its applicability across a broader range of real-world conditions.

## REFERENCES

- [1] M. Coppola, K. N. McGuire, C. De Wagter, and G. C. H. E. de Croon, “A survey on swarming with micro air vehicles: Fundamental challenges and constraints,” *Front. Robot. AI*, vol. 7, 2020, Art. no. 18.
- [2] D. Floreano and R. J. Wood, “Science, technology and the future of small autonomous drones,” *Nature*, vol. 521, no. 7553, pp. 460–466, 2015.
- [3] E. Soria, F. Schiano, and D. Floreano, “Predictive control of aerial swarms in cluttered environments,” *Nature Mach. Intell.*, vol. 3, no. 6, pp. 545–554, 2021.
- [4] X. Zhou et al., “Swarm of micro flying robots in the wild,” *Sci. Robot.*, vol. 7, no. 66, 2022, Art. no. eabm5954.
- [5] S. Hauert et al., “Reynolds flocking in reality with fixed-wing robots: Communication range vs. maximum turning rate,” in *Proc. IEEE/RSJ Int. Conf. Intell. Robots Syst.*, 2011, pp. 5015–5020.
- [6] G. Vásárhelyi, C. Virág, G. Somorjai, T. Nepusz, A. E. Eiben, and T. Vicsek, “Optimized flocking of autonomous drones in confined environments,” *Sci. Robot.*, vol. 3, no. 20, 2018, Art. no. eaat3536.
- [7] F. Schilling, J. Lecoeur, F. Schiano, and D. Floreano, “Learning vision-based cohesive flight in drone swarms,” 2018, *arXiv:1809.00543*.
- [8] T. Cieslewski, S. Choudhary, and D. Scaramuzza, “Data-efficient decentralized visual SLAM,” in *Proc. IEEE Int. Conf. Robot. Autom.*, 2018, pp. 2466–2473.
- [9] I. D. Couzin, J. Krause, N. R. Franks, and S. A. Levin, “Effective leadership and decision-making in animal groups on the move,” *Nature*, vol. 433, no. 7025, pp. 513–516, 2005.
- [10] H. Hildenbrandt, C. Carere, and C. K. Hemelrijk, “Self-organized aerial displays of thousands of starlings: A model,” *Behav. Ecol.*, vol. 21, no. 6, pp. 1349–1359, 2010.
- [11] M. Nagy, Z. Ákos, D. Biro, and T. Vicsek, “Hierarchical group dynamics in pigeon flocks,” *Nature*, vol. 464, no. 7290, pp. 890–893, 2010.
- [12] M. Yomosa, T. Mizuguchi, G. Vásárhelyi, and M. Nagy, “Coordinated behaviour in pigeon flocks,” *PLoS One*, vol. 10, no. 10, 2015, Art. no. e0140558.

- [13] J. D. Davidson, M. M. Sosna, C. R. Twomey, V.H. Sridhar, S. P. Leblanc, and I. D. Couzin, "Collective detection based on visual information in animal groups," *J. Roy. Soc. Interface*, vol. 18, no. 180, 2021, Art. no. 20210142.
- [14] A. Strandburg-Peshkin et al., "Visual sensory networks and effective information transfer in animal groups," *Curr. Biol.*, vol. 23, no. 17, pp. R709–R711, 2013.
- [15] D. J. Pearce and M. S. Turner, "Density regulation in strictly metric-free swarms," *New J. Phys.*, vol. 16, no. 8, 2014, Art. no. 082002.
- [16] T. Vicsek, A. Czirók, E. Ben-Jacob, I. Cohen, and O. Shochet, "Novel type of phase transition in a system of self-driven particles," *Phys. Rev. Lett.*, vol. 75, no. 6, 1995, Art. no. 1226.
- [17] I. D. Couzin, J. Krause, R. James, G. D. Ruxton, and N. R. Franks, "Collective memory and spatial sorting in animal groups," *J. Theor. Biol.*, vol. 218, no. 1, pp. 1–11, 2002.
- [18] A. Huth and C. Wissel, "The simulation of the movement of fish schools," *J. Theor. Biol.*, vol. 156, no. 3, pp. 365–385, 1992.
- [19] F. Schilling, F. Schiano, and D. Floreano, "Vision-based drone flocking in outdoor environments," *IEEE Robot. Autom. Lett.*, vol. 6, no. 2, pp. 2954–2961, Apr. 2021.
- [20] F. Schilling, J. Lecoeur, F. Schiano, and D. Floreano, "Learning vision-based flight in drone swarms by imitation," *IEEE Robot. Autom. Lett.*, vol. 4, no. 4, pp. 4523–4530, Oct. 2019.
- [21] D. L. Altshuler and M.V. Srinivasan, "Comparison of visually guided flight in insects and birds," *Front. Neurosci.*, vol. 12, 2018, Art. no. 157.
- [22] C. Ellington, "Insects versus birds: The great divide," in *Proc. 44th AIAA Aerosp. Sci. Meeting Exhib.*, 2006, Art. no. AIAA 2006-35.
- [23] I. K. Erunsal, A. Martinoli, and R. Ventura, "Decentralized nonlinear model predictive control for 3D formation of multirotor micro aerial vehicles with relative sensing and estimation," in *Proc. Int. Symp. Multi-Robot Multi-Agent Syst.*, 2019, pp. 176–178.
- [24] T. J. Stastny, A. Dash, and R. Siegwart, "Nonlinear MPC for fixed-wing UAV trajectory tracking: Implementation and flight experiments," in *Proc. AIAA Guid., Navigat., Control Conf.*, 2017, Art. no. 1512.
- [25] X. Wang, Y. Yu, and Z. Li, "Distributed sliding mode control for leader-follower formation flight of fixed-wing unmanned aerial vehicles subject to velocity constraints," *Int. J. Robust Nonlinear Control*, vol. 31, no. 6, pp. 2110–2125, 2021.
- [26] J. Tang, F. Zhu, and M. A. Piera, "A causal encounter model of traffic collision avoidance system operations for safety assessment and advisory optimization in high-density airspace," *Transp. Res. C, Emerg. Technol.*, vol. 96, pp. 347–365, 2018.
- [27] M. Saska, D. Hert, T. Baca, V. Kratky, and T. Nascimento, "Formation control of unmanned micro aerial vehicles for straitened environments," *Auton. Robots*, vol. 44, pp. 991–1008, 2020.
- [28] L. Li, W. Sheng, and C. Hu, "Research on formation keeping of multi-rotor UAVs based on improved virtual structure method," *J. Phys.: Conf. Ser.*, vol. 1631, 2020, Art. no. 012106.
- [29] A. Askari, M. Mortazavi, and H. A. Talebi, "UAV formation control via the virtual structure approach," *J. Aerosp. Eng.*, vol. 28, no. 1, 2015, Art. no. 04014047.
- [30] J. Alonso-Mora, E. Montijano, T. Nägeli, O. Hilliges, M. Schwager, and D. Rus, "Distributed multi-robot formation control in dynamic environments," *Auton. Robots*, vol. 43, pp. 1079–1100, 2019.
- [31] K. Choutri, M. Lagha, and L. Dala, "Distributed obstacles avoidance for UAVs formation using consensus-based switching topology," *Int. J. Comput. Digit. Syst.*, vol. 8, no. 2, pp. 167–178, 2019.
- [32] X. Dong, Y. Li, C. Lu, G. Hu, Q. Li, and Z. Ren, "Time-varying formation tracking for UAV swarm systems with switching directed topologies," *IEEE Trans. Neural Netw. Learn. Syst.*, vol. 30, no. 12, pp. 3674–3685, Dec. 2019.
- [33] J. Wang, L. Han, X. Li, X. Dong, Q. Li, and Z. Ren, "Time-varying formation of second-order discrete-time multi-agent systems under non-uniform communication delays and switching topology with application to UAV formation flying," *IET Control Theory Appl.*, vol. 14, no. 14, pp. 1947–1956, 2020.
- [34] R. Xue, J. Song, and G. Cai, "Distributed formation flight control of multi-UAV system with nonuniform time-delays and jointly connected topologies," *Proc. Inst. Mech. Eng., G: J. Aerosp. Eng.*, vol. 230, no. 10, pp. 1871–1881, 2016.
- [35] C. W. Reynolds, "Flocks, herds and schools: A distributed behavioral model," in *Proc. 14th Annu. Conf. Comput. Graph. Interact. Techn.*, 1987, pp. 25–34.
- [36] H. Qiu and H. Duan, "A multi-objective pigeon-inspired optimization approach to UAV distributed flocking among obstacles," *Inf. Sci.*, vol. 509, pp. 515–529, 2020.
- [37] E. Soria, F. Schiano, and D. Floreano, "The influence of limited visual sensing on the Reynolds flocking algorithm," in *Proc. IEEE 3rd Int. Conf. Robot. Comput.*, 2019, pp. 138–145.
- [38] R. G. Braga, R. C. Da Silva, A. C. Ramos, and F. Mora-Camino, "Collision avoidance based on Reynolds rules: A case study using quadrotors," in *Proc. 14th Int. Conf. Inf. Technol.*, 2018, pp. 773–780.
- [39] H. Ye, X. Zhou, Z. Wang, C. Xu, J. Chu, and F. Gao, "TGK-planner: An efficient topology guided kinodynamic planner for autonomous quadrotors," *IEEE Robot. Autom. Lett.*, vol. 6, no. 2, pp. 494–501, Apr. 2021.
- [40] J. Tordesillas and J. P. How, "MADER: Trajectory planner in multiagent and dynamic environments," *IEEE Trans. Robot.*, vol. 38, no. 1, pp. 463–476, Feb. 2022.
- [41] J. Tordesillas, B. T. Lopez, and J. P. How, "Faster: Fast and safe trajectory planner for flights in unknown environments," in *Proc. IEEE/RSJ Int. Conf. Intell. Robots Syst.*, 2019, pp. 1934–1940.
- [42] X. Zhou, J. Zhu, H. Zhou, C. Xu, and F. Gao, "EGO-swarm: A fully autonomous and decentralized quadrotor swarm system in cluttered environments," in *Proc. IEEE Int. Conf. Robot. Autom.*, 2021, pp. 4101–4107.
- [43] S. S. Mansouri, P. Karvelis, C. Kanellakis, D. Kominiak, and G. Nikolakopoulos, "Vision-based MAV navigation in underground mine using convolutional neural network," in *Proc. 45th Annu. Conf. IEEE Ind. Electron. Soc.*, 2019, vol. 1, pp. 750–755.
- [44] S.-C. Han and H. Bang, "Proportional navigation-based optimal collision avoidance for UAVs," in *Proc. 2nd Int. Conf. Auton. Robots Agents*, 2009, pp. 13–15.
- [45] T. Baca, D. Hert, G. Loianno, M. Saska, and V. Kumar, "Model predictive trajectory tracking and collision avoidance for reliable outdoor deployment of unmanned aerial vehicles," in *Proc. IEEE/RSJ Int. Conf. Intell. Robots Syst.*, 2018, pp. 6753–6760.
- [46] A. Grancharova, E. I. Grøtli, D.-T. Ho, and T. A. Johansen, "UAVs trajectory planning by distributed MPC under radio communication path loss constraints," *J. Intell. Robot. Syst.*, vol. 79, pp. 115–134, 2015.
- [47] C. E. Luis, M. Vukosavljev, and A. P. Schoellig, "Online trajectory generation with distributed model predictive control for multi-robot motion planning," *IEEE Robot. Autom. Lett.*, vol. 5, no. 2, pp. 604–611, Apr. 2020.
- [48] T. Keviczky, F. Borrelli, K. Fregene, D. Godbole, and G. J. Balas, "Decentralized receding horizon control and coordination of autonomous vehicle formations," *IEEE Trans. Control Syst. Technol.*, vol. 16, no. 1, pp. 19–33, Jan. 2008.
- [49] R. Van Parys and G. Pipeleers, "Distributed MPC for multi-vehicle systems moving in formation," *Robot. Auton. Syst.*, vol. 97, pp. 144–152, 2017.
- [50] B. Lindqvist, S. S. Mansouri, A.-A. Agha-Mohammadi, and G. Nikolakopoulos, "Nonlinear MPC for collision avoidance and control of UAVs with dynamic obstacles," *IEEE Robot. Autom. Lett.*, vol. 5, no. 4, pp. 6001–6008, Oct. 2020.
- [51] Y. Kuwata and J. P. How, "Robust cooperative decentralized trajectory optimization using receding horizon MILP," in *Proc. IEEE Amer. Control Conf.*, 2007, pp. 522–527.
- [52] M. Kamel, J. Alonso-Mora, R. Siegwart, and J. Nieto, "Robust collision avoidance for multiple micro aerial vehicles using nonlinear model predictive control," in *Proc. IEEE/RSJ Int. Conf. Intell. Robots Syst.*, 2017, pp. 236–243.

- [53] G. R. Martin, "Visual fields in woodcocks scolopax rusticola (scolopacidae; charadriiformes)," *J. Comp. Physiol. A*, vol. 174, pp. 787–793, 1994.
- [54] Martin, "The eye of a passeriform bird, the European starling (*Sturnus vulgaris*): Eye movement amplitude, visual fields and schematic optics," *J. Comp. Physiol. A*, vol. 159, pp. 545–557, 1986.
- [55] G. Netzer, Y. Yarom, and G. Ariel, "Heterogeneous populations in a network model of collective motion," *Phys. A: Statist. Mech. Appl.*, vol. 530, 2019, Art. no. 121550.
- [56] B. Afsharizand, P. H. Chaghoei, A. A. Kordbacheh, A. Trufanov, and G. Jafari, "Market of stocks during crisis looks like a flock of birds," *Entropy*, vol. 22, no. 9, 2020, Art. no. 1038.
- [57] Y.-J. Li, S. Wang, Z.-L. Han, B.-M. Tian, Z.-D. Xi, and B.-H. Wang, "Optimal view angle in the three-dimensional self-propelled particle model," *Europhys. Lett.*, vol. 93, no. 6, 2011, Art. no. 68003.
- [58] Y. Jia, Q. Li, and Z. Zhang, "Accelerating emergence of aerial swarm," *Appl. Sci.*, vol. 10, no. 22, 2020, Art. no. 7986.
- [59] S.-H. Lee and V. T. Ngo, "Effect of vision angle on the phase transition in flocking behavior of animal groups," *Phys. Rev. E*, vol. 92, no. 3, 2015, Art. no. 032716.
- [60] Q. Li, L. Zhang, Y. Jia, T. Lu, and X. Chen, "Modeling, analysis, and optimization of three-dimensional restricted visual field metric-free swarms," *Chaos, Solitons Fractals*, vol. 157, 2022, Art. no. 111879.
- [61] B.-M. Tian, H.-X. Yang, W. Li, W.-X. Wang, B.-H. Wang, and T. Zhou, "Optimal view angle in collective dynamics of self-propelled agents," *Phys. Rev. E*, vol. 79, no. 5, 2009, Art. no. 052102.
- [62] A. M. Calvao and E. Brigatti, "The role of neighbours selection on cohesion and order of swarms," *PLoS One*, vol. 9, no. 5, 2014, Art. no. e94221.
- [63] H. Duan and X. Zhang, "Phase transition of vortexlike self-propelled particles induced by a hostile particle," *Phys. Rev. E*, vol. 92, no. 1, 2015, Art. no. 012701.
- [64] E. Kaufmann, A. Loquercio, R. Ranftl, M. Müller, V. Koltun, and D. Scaramuzza, "Deep drone acrobatics," *Proc. Robot.: Sci. Syst. Conf.*, 2020.
- [65] D. Mellinger and V. Kumar, "Minimum snap trajectory generation and control for quadrotors," in *Proc. IEEE Int. Conf. Robot. Autom.*, 2011, pp. 2520–2525.
- [66] C.-Y. Wang, A. Bochkovskiy, and H.-Y. M. Liao, "YOLOv7: Trainable bag-of-freebies sets new state-of-the-art for real-time object detectors," in *Proc. IEEE/CVF Conf. Comput. Vis. Pattern Recognit.*, 2023, pp. 7464–7475.
- [67] R. Olfati-Saber and R. M. Murray, "Consensus problems in networks of agents with switching topology and time-delays," *IEEE Trans. Autom. Control*, vol. 49, no. 9, pp. 1520–1533, Sep. 2004.
- [68] M. Ballerini et al., "Interaction ruling animal collective behavior depends on topological rather than metric distance: Evidence from a field study," *Proc. Nat. Acad. Sci.*, vol. 105, no. 4, pp. 1232–1237, 2008.
- [69] J. A. Andersson, J. Gillis, G. Horn, J. B. Rawlings, and M. Diehl, "CasADI: A software framework for nonlinear optimization and optimal control," *Math. Program. Comput.*, vol. 11, pp. 1–36, 2019.

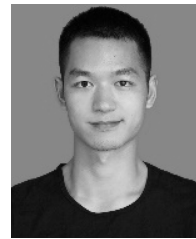


**Jun Tang** received the Ph.D. degree in logistic systems, causal modeling, state space, air traffic management and discrete event simulation (DES) from the Technical Innovation Cluster on Aeronautical Management Group, Universitat Autònoma de Barcelona, Bellaterra, Spain in 2015.

He is currently an Associate Professor with the Science and Technology on Information Systems Engineering Laboratory, National University of Defense Technology, Changsha, China.

He has been very active in the simulation community, organizing as general co-chair for several international conferences. He acted as one of the main participants playing an important role in the FP7 European project "INnovative TEchnologies and Researches for a new Airport Concept towards Turnaround coordinatION (INTERACTION)" with collaboration of Airbus. His research interests include logistic systems, causal modeling, state space, air traffic management, and discrete-event simulation.

Dr. Tang was the recipient of the William Sweet Smith Prize in 2015.



**Yu Wan** received the B.E. degree in Multiple-UAV cooperation and M.E. degree in Visual navigation 2017 and 2020, respectively, from the National University of Defense Technology, Changsha, China, where he is currently working toward the Ph.D. degree in Motion Planning, Imitation Learning.

During the M.E. degree, he studied the system engineering and the operation research. He then started to work on theories and methods of collision avoidance of aircraft. His research interests

include air traffic management and unmanned aerial vehicle systems, such as collision avoidance of aircraft.



**Songyang Lao** received the B.S. degree in information system engineering and the Ph.D. degree in system engineering from the National University of Defense Technology, Changsha, China, in 1990 and 1996, respectively.

In 1996, he joined, as a Faculty Member, the National University of Defense Technology, where he is currently a Professor with the School of Information System and Management. From 2004 to 2005, he was a Visiting Scholar with Dublin City University, Dublin, Ireland. His current research interests include image processing and video analysis and human-computer interaction.



**Zipeng Zhao** received the B.E. degree in Multiple-UAV cooperation from the College of Information Science and Engineering, Lanzhou University, Lanzhou, China, in 2022. He is currently working toward the Ph.D. degree in Trajectory Planning, Reinforcement learning with the College of Systems Engineering, National University of Defense Technology, Changsha, China.

His research interests include unmanned aerial vehicle systems and path planning.